Cerebral Cortex July 2015;25:1835–1841
doi:10.1093/cercor/bht424
Advance Access publication January 15, 2014

Maturation of Cortico-Subcortical Structural Networks—Segregation and Overlap of Medial Temporal and Fronto-Striatal Systems in Development

Kristine B. Walhovd[1], Christian K. Tamnes[1], Atle Bjørnerud[1,2], Paulina Due-Tønnessen[1,2], Dominic Holland[3], Anders M. Dale[3] and Anders M. Fjell[1]

[1]Department of Psychology, Research Group for Lifespan Changes in Brain and Cognition (LCBC), University of Oslo, Oslo, Norway, [2]Oslo University Hospital, Rikshospitalet, Oslo, Norway and [3]Multimodal Imaging Laboratory, Departments of Radiology and Neuroscience, University of California San Diego, La Jolla, CA 92093, USA

Address correspondence to Dr Kristine B. Walhovd, Department of Psychology, University of Oslo, PO Box 1094 Blindern, 0317 Oslo, Norway. Email: k.b.walhovd@psykologi.uio.no

The brain consists of partly segregated neural circuits within which structural convergence and functional integration occurs during development. The relationship of structural cortical and subcortical maturation is largely unknown. We aimed to study volumetric development of the hippocampus and basal ganglia (caudate, putamen, pallidum, accumbens) in relation to volume changes throughout the cortex. Longitudinal MRI data were obtained across a mean interval of 2.6 years in 85 participants with an age range of 8–19 years at study start. Left and right subcortical changes were related to cortical change vertex-wise in the ipsilateral hemisphere with general linear models with age, sex, interval between scans, and mean cortical volume change as covariates. Hippocampal–cortical change relationships centered on parts of the Papez circuit, including entorhinal, parahippocampal, and isthmus cingulate areas, and lateral temporal, insular, and orbitofrontal cortices in the left hemisphere. Basal ganglia-cortical change relationships were observed in mostly nonoverlapping and more anterior cortical areas, all including the anterior cingulate. Other patterns were unique to specific basal ganglia structures, including pre-, post-, and paracentral patterns relating to putamen change. In conclusion, patterns of cortico-subcortical development as assessed by morphometric analyses in part map out segregated neural circuits at the macrostructural level.

Keywords: cerebral cortex, development, MRI, neural networks, subcortical volumes

Introduction

A basic tenet in neuroscience is that the brain does not consist of isolated areas subserving specific functions on their own, but rather of sets of interconnected regions, forming segregated neural circuits. One of the major challenges of cognitive neuroscience is to understand functional anatomy based on these structural substrates (Park and Friston 2013). Structural convergence and functional integration occur within, rather than between, each of the identified segregated circuits (Alexander et al. 1990). This principle is assumed to apply also to brain development, but evidence is incomplete at best. Recently, regional differences in cortical as well as subcortical maturation (Sowell et al. 2002; Lenroot and Giedd 2006; Østby et al. 2009; Tamnes et al. 2010, 2013 Raznahan, Lerch, et al. 2011; Raznahan, Shaw, et al. 2011; Brain Development Cooperative Group 2012; Brown et al. 2012; Alexander-Bloch et al. 2013) have been mapped in school age and beyond. Patterns of morphometric correlations and anticorrelations within the cortical mantle in development are emerging (Lerch et al. 2006; Raznahan, Lerch, et al. 2011; Alexander-Bloch et al. 2013; Evans 2013). Very recently, Albaugh et al. (2013) demonstrated that regional cerebral cortical thickness was inversely related to amygdalar volume in healthy youths, indicating recapitulation of functional reciprocity between limbic and dorsal neocortical regions from a purely structural standpoint. To understand the hitherto identified region-specific maturational changes, it is now critical that cortical and subcortical maturation are studied in relation in the same individuals over time, according to the putative interconnections between areas. Current prime candidates for such investigations are the hippocampi and basal ganglia, which form subcortical–cortical circuits critical to development of major cognitive functions (Alexander et al. 1990; Shah et al. 2012) and, hence, their maturation is of outmost importance.

The Papez circuit, critical to episodic memory, begins in the hippocampus, continues into the fornix to the mammillary bodies, via the mammillothalamic tract to the anterior nucleus of the thalamus, connecting to the cingulum by means of anterior thalamic radiations (Shah et al. 2012). Prefrontal basal ganglia-thalamocortical circuits include dorsolateral prefrontal (DLPFC) and lateral orbitofrontal (LOFC) cortical projections to the caudate. The precuneus, which is interconnected with the DLPFC, has also been shown to project to the dorsolateral head of the caudate (Alexander et al. 1986, 1990). These circuits have been implicated in working memory and task switching capabilities (Lovstad et al. 2012). In primates, the basal ganglia motor pathways are focused primarily on the putamen, which receives connections from primary motor, premotor, and somatosensory cortex (Alexander et al. 1990). Evidence to date indicate that the putamen is implicated in balancing of activation and inhibition circuitry (Disbrow et al. 2013). Finally, nucleus accumbens is part of the ventral striatum and a limbic circuit receiving projections form the anterior cingulate, medial orbitofrontal cortices, and widespread sources within the temporal lobe. All of these basal ganglia structures project via, among other areas, pallidal, and thalamic segments back to cortical areas, closing the circuits (Alexander et al. 1990). It should be noted that, while there are specific circuits with dedicated functions, recent evidence has also pointed to integration across limbic and basal ganglia cortical circuits in regulatory systems of the brain (Haber and Knutson 2010; Milad and Rauch 2012). There are indications that corticostriatal loops are more integrated within the striatum and thalamus than previously thought (Milad and Rauch 2012). The above-described circuits support several complex cognitive processes, including episodic memory and executive

functioning both in normally developing children and in neuropsychiatric developmental conditions such as schizophrenia, attention-deficit/ hyperactivity, and obsessive–compulsive disorder and have a protracted development in childhood and adolescence (Robbins 2007; Ghetti and Bunge 2012). Importantly, the foundations of a range of developmental disorders are thought to arise in deficient regulation of cortico-subcortical circuitry (Shepherd 2013). Such deficits may likely have structural maturational causes, and delineating the normal structural synchronization of cortico-subcortical maturation appears essential to understanding and identifying problems in critical circuitry.

We present analyses of longitudinal MRI data from 85 children and adolescents in the age range 8–22 years, delineating patterns of coordinated change across subcortical and regional cortical volumes. We used a novel unbiased method to quantify volumetric change (Holland and Dale 2011) that is highly sensitive to even subtle changes over short time periods (Murphy et al. 2010; Holland et al. 2012; Tamnes et al. 2013). Image segmentation and parcellation was done to obtain change estimates throughout the brain. As outlined above, the main objective of this study is to investigate how the hippocampus and basal ganglia develop in coordination with the cerebral cortex. The pattern of change in relation to these structures is likely widespread, but hitherto uninvestigated and needs to be tested anatomically unconstrained throughout the cortical mantle. Hence, the hippocampus, caudate, putamen, pallidum, and accumbens area were chosen for unbiased analyses of coordinated cortico-subcortical development. We tentatively hypothesized that patterns of cortical change related to hippocampal and basal ganglia change would essentially map onto major established circuits for episodic memory and executive function, respectively. Thus, the following specific hypotheses were put forth: 1) Hippocampal volume change will relate selectively to cortical volume change in the Papez circuit. More specifically, we expect hippocampal change in development to relate closely to temporal and cingulate cortical changes. 2) Basal ganglia change will relate selectively to frontal and parietal cortical changes. For instance, we expect volume changes to be systematically related in the caudate, DLPFC, and precuneus, in the accumbens and anterior cingulate, and a selective relationship between volume change in the putamen and motor areas of the cortex. 3) To the extent that there is also some integration across circuits, we also expect to see partly overlapping patterns of structural change, especially among structures within the basal ganglia and frontal cortical areas.

Materials and Methods

Sample

The sample of children and adolescents was drawn from the longitudinal project "Neurocognitive Development" (Østby et al. 2009; Tamnes et al. 2010, 2013) run by Research Group for Lifespan Changes in Brain and Cognition (LCBC), Department of Psychology, University of Oslo. The study was approved by the Regional Committee for Medical and Health Research Ethics. Typically developing children and adolescents aged 8–19 years were recruited though newspaper ads and local schools. Written informed consent was obtained from all participants older than 12 years of age and from a parent of participants under 16 years of age. Oral informed consent was given by participants under 12 years of age. Parents and participants aged 16 years or older were at both time-points screened with separate standardized health interviews to ascertain eligibility. Participants were required to be right handed, fluent Norwegian speakers, have normal or corrected to normal vision and hearing, not have history of injury or disease known to affect central nervous system (CNS) function, including neurological or psychiatric illness or serious head trauma, not be under psychiatric treatment, not use psychoactive drugs known to affect CNS functioning, not have had complicated or premature birth, and not have MRI contraindications. Additionally, all scans were evaluated by a neuroradiologist at both time-points and required to be deemed free of significant injuries or conditions.

At time-point 1 (tp1), 111 participants satisfied these criteria and had adequate processed and quality checked MRI data. Eighteen participants did not want to or were unable to participate at time-point 2 (tp2), 2 were unable to locate, 3 had dental braces, and 3 were excluded due to neurological or psychiatric conditions. Thus, at tp2, 85 participants (38 females) underwent a second MRI scan. Mean age at tp1 for this final sample was 13.7 years (SD = 3.4, range = 8.2–19.4) and mean IQ, as assessed by the Wechsler Abbreviated Scale of Intelligence (WASI) (Wechsler 1999), was 109.0 (SD = 11.4, range = 82–141). Mean age at tp2 was 16.3 years (SD = 3.4, range = 10.8–21.9), and mean IQ was 112.5 (SD = 10.5, range = 87–136). Mean interval between the 2 scanning sessions was 2.6 years (SD = 0.2, range = 2.4–3.2). The length of the interval was not related to age ($r = -0.03$, $P > 0.500$) and not different for girls and boys ($T = 0.413$, $P > 0.500$).

MRI Acquisition

Imaging data were acquired using a 12-channel head coil on a 1.5-T Siemens Avanto scanner (Siemens Medical Solutions, Erlangen, Germany). The pulse sequences used for morphometry analysis were 2 repeated T_1-weighted magnetization prepared rapid gradient echo (MPRAGE) sequences, with the following parameters: repetition time (TR)/echo time (TE)/time to inversion (TI)/flip angel (FA) = 2400 ms/3.61 ms/1000 ms/8°, matrix 192 × 192, field of view = 192. Each volume consisted of 160 sagittal slices with voxel size 1.25 × 1.25 × 1.20 mm. Acquisition time for each sequence was 7 min, 42 s. Two to four runs of this sequence were acquired for each participant at each time-point. Scans were manually inspected, and scans with major movement artifacts were excluded, while the remaining scans were averaged during postprocessing in order to increase the signal-to-noise ratio. Mean number of scans averaged was 2.2 (SD = 0.4) at both time-points. The protocol also included a 176 slices sagittal 3D T_2-weighted turbo spin-echo sequence (TR/TE = 3390/388 ms), and a 25 slices coronal FLAIR sequence (TR/TE = 7000–9000/109 ms) used for clinical assessment.

MRI Analyses

Image processing and analyses were performed at the Multimodal Imaging Laboratory, University of California, San Diego. The raw data were reviewed for quality, and automatically corrected for spatial distortion due to gradient nonlinearity (Jovicich et al. 2006) and B_1 field inhomogeneity (Sled et al. 1998). The 2 image volumes for each participant were co-registered, averaged and resampled to isotropic 1-mm voxels. Neuroanatomical segmentation (Fischl et al. 2002) and cortical surface reconstruction (Fischl, Sereno, Dale 1999; Fischl, Sereno, Tootell, et al. 1999; Fischl and Dale 2000) and parcellation (Fischl et al. 2004; Desikan et al. 2006) were performed using the newest version of the FreeSurfer software package available at the time of analysis (version 5.1.0; Martinos Center for Biomedical Imaging, Boston, MA, USA). In the brain segmentation, every voxel is given a unique label, meaning that the volumes reported here are from nonoverlapping areas. For example, the caudate and the accumbens area are distinct areas. See Figure 1 for an example of the subcortical segmentations. The subcortical segmentation and surface reconstruction and parcellation procedures are run automatically, but require supervision of the accuracy of spatial registration and tissue segmentations. All segmentations and parcellations were inspected for accuracy and minor manual edits were performed by a trained operator on the baseline images for nearly all subjects, usually restricted to removal of nonbrain tissue included within the cortical boundary.

Longitudinal changes in brain structure measures were quantified by Quarc (Quantitative anatomical regional change) (Holland and Dale

2011; Holland et al. 2012), developed at the Multimodal Imaging Laboratory, University of California, San Diego. For each participant, dual 3D follow-up structural scans were rigid-body aligned, averaged, and affine aligned to the participant's baseline. A deformation field was calculated from a nonlinear registration (Holland and Dale 2011). The images are heavily blurred (smoothed), making them almost identical, and a merit or potential function calculated. This merit function expresses the intensity difference between the images at each voxel, and depends on the displacement field for the voxel centers of the image being transformed; it is also regularized to keep the displacement field spatially smooth. The merit function by design will have a minimum when the displacement field induces a good match between the images. It is minimized efficiently using standard numerical methods. Having found a displacement field for the heavily blurred pair of images, the blurring is reduced and the procedure repeated, thus iteratively building up a better displacement field. Two important additions to this are 1) applying the final displacement field to the image being transformed, then nonlinearly registering the resultant image to the same target, and finally tracing back through the displacement field thus calculated to find the net displacement field and 2) restricting the displacement fields to regions of interest and zooming when structures are separated by only a voxel or 2. These additional features enable very precise registration involving large or subtle deformations, even at small spatial scales with low boundary contrast. Zooming was done for the region encompassing the hippocampus, amygdala, and temporal horn of the lateral ventricles, left and right independent. Forward and reverse registrations were performed and averaged to avoid bias in change estimates. After a preparatory registration, 5 iterations of nonlinear registration were performed to align source to target. Although large deformations are allowed by multiple nonlinear registration (or relaxation) steps, nonphysical deformations are precluded because at each level of blurring the image undergoing deformation is restricted to conform to the target. Note that calculating the deformation field does not depend on initially segmenting tissue. This deformation field was used to align scans at the subvoxel level. Furthermore, this was combined with image segmentation and parcellation to obtain volume change estimates in a large number of cortical and subcortical regions. The processing pipeline can be shortly summarized as follows: 1) raw dicom --> 2) gradient-warp correction --> 3) baseline segmentation --> 4) quarc --> 5) volume change field statistically analyzed. Step 4 includes 1) affine registration of source to target, 2) local (B_1 field) intensity normalization, 3) multiple nonlinear registration steps, 4) zooming, 5) repetition of 1–4 but target to source, and 6) combination of the forward and the reverse solution. For additional information, interested readers are referred to the methodological papers referenced above, in particular (Holland and Dale 2011), where step 1–4 are described in detail.

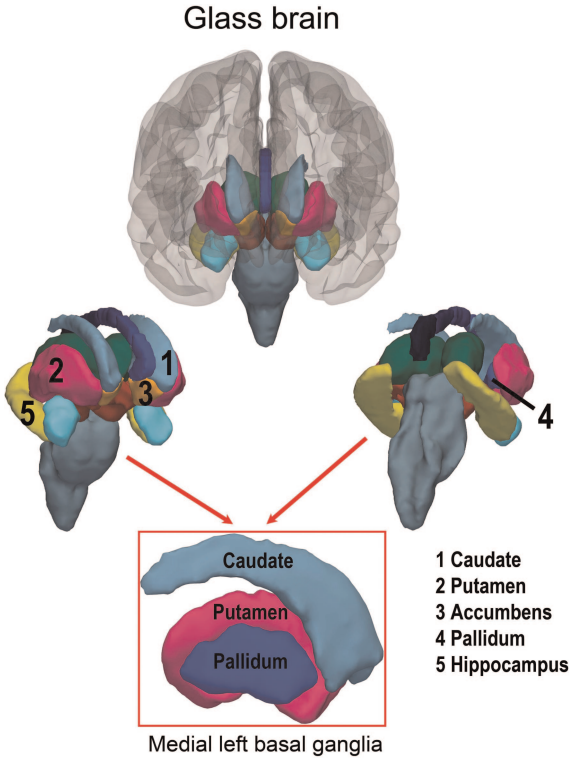

Figure 1. Segmentation of subcortical structures shown in 3D. The figure is based on the segmentation results of the average of 208 healthy volunteers.

The second time-point was used as baseline, as it is reasonable to assume that there is less motion distortion with older age in developmental samples. To ease interpretation of the results, the direction of all effects were inversed in the surface illustrations. Freesurfer subcortical segmentation, cortical surface reconstructions and parcellation labels from the second time-point images were used to extract average volume change from Quarc for each ROI and vertex. For select ROIs, annual percentage volume change from tp 1 was calculated prior to statistical analyses. The FreeSurfer segmentation and parcellation techniques were used as they allowed us to map longitudinal changes in multiple subcortical structures and anatomically meaningful cortical regions. Quarc has previously been applied to serial pairs of scans from both young and elderly participants and been proven to be highly sensitive to even subtle changes over short time periods (Fjell et al. 2009; Murphy et al. 2010; Holland et al. 2012; Tamnes et al. 2013).

Statistical Analysis

General volume changes with age in the present sample have been presented elsewhere (Tamnes et al. 2013). Only means and standard deviations for annual percent change for left and right hemisphere hippocampal and basal ganglia segmentations and select cortical parcellations of the hypothesized circuits are provided here as a backdrop for the present analyses on coordination of subcortical and cortical changes (see Table 1). In this sample, volume change across age has been shown to be monotonously negative in the hippocampus, basal ganglia, and cerebral cortex, with no effect of sex on cortical change. Due to this, and the relatively small sample size, square of age was not included in the analyses. Age, sex, interval between scans, mean cortical volume change calculated by averaging mean change at each vertex for each participant, as well as the interaction of sex with these covariates were included as covariates. Left and right hippocampal and basal ganglia change were related to cortical change vertex-wise in the ipsilateral hemisphere with general linear models as implemented in FreeSurfer with age, sex, interval between scans, and mean cortical volume change within the respective hemisphere as covariates. All subcortical volumes entered in analyses involved unilateral volumes. Corrections for multiple comparisons were done for the hemisphere analyzed. The results were tested against an empirical null distribution of maximum cluster size across 10 000 iterations using Z Monte Carlo simulations as

Table 1

Means and standard deviations for annual percent volume change for left and right hemisphere hippocampal and basal segmentations and select cortical parcellations of the hypothesized circuits

ROI	Mean (SD) percent annual change	
	Left	Right
Hippocampus	−0.18 (0.38)	−0.14 (0.38)
Caudate	−0.83 (0.48)	−0.80 (0.48)
Putamen	−0.59 (0.36)	−0.60 (0.38)
Pallidum	−0.20 (0.36)	−0.20 (0.38)
Accumbens area	−0.64 (0.58)	−0.59 (0.50)
Enthorinal	−0.14 (0.07)	0.05 (0.84)
Parahippocampal	−0.66 (0.59)	−0.71 (0.55)
Posterior cingulate	−1.14 (0.51)	−1.09 (0.50)
Isthmus cingulate	−1.04 (0.49)	−0.95 (0.49)
Caudal anterior cingulate	−0.87 (0.46)	−0.74 (0.48)
Rostral anterior cingulate	−0.81 (0.57)	−0.65 (0.48)
Precuneus	−1.40 (0.56)	−1.32 (0.56)
Medial orbitofrontal	−0.85 (0.51)	−0.86 (0.51)
Lateral orbitofrontal	−0.83 (0.49)	−0.85 (0.52)
Paracentral	−0.85 (0.60)	−0.71 (0.56)
Precentral	−0.47 (0.63)	−0.52 (0.64)
Postcentral	−0.92 (0.56)	−0.93 (0.54)

implemented in FreeSurfer (Hayasaka and Nichols 2003; Hagler et al. 2006) synthesized with a cluster-forming threshold of $P < 0.05$ (two-sided), yielding clusters corrected for multiple comparisons across the surface. Results were displayed on a semi-inflated template brain. To restrict the number of statistical tests, only ipsilateral relationships were tested. As mean cortical change was entered as a covariate, the resulting statistical maps show areas where relationships are significantly stronger and weaker than the mean. Relationships significantly weaker than the mean should not be seen as negative per se, as all identified relationships between subcortical and cortical change were in the same direction and positive (for a sample of relationships observed when mean cortical change was not co-varied for, see Supplementary Fig. 1).

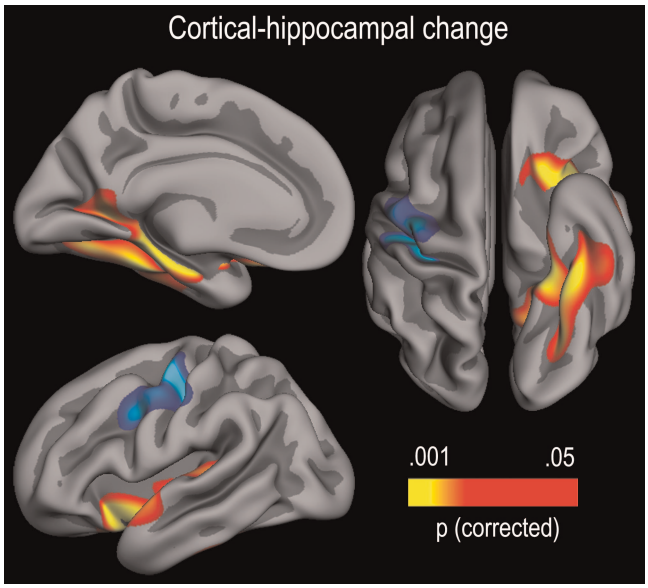

Figure 2. Coordinated hippocampal–cortical volume change. Relationships between hippocampal change and cortical change, with sex, age, follow-up interval, and mean cortical change as covariates. The results were corrected for multiple comparisons by Monte Carlo simulations, and only clusters with a cluster-wise $P < 0.05$ are shown. Red-yellow colors denote relationships significantly stronger than the mean, while blue-cyan colors indicate relationships significantly weaker than the mean. No relationships survived corrections in the right hemisphere.

Results

The results are displayed in Figure 2 for the hippocampus, and in Figure 3 for each basal ganglia structure. In Figures 3 and 4, overlap among structures in patterns of cortical volume change is also indicated. For the hippocampus, only relationships between left hemisphere cortical change and left hippocampus change were seen after controlling for mean cortical change. Relationships of change stronger than mean cortical change were mostly observed in the parahippocampal and fusiform cortices, extending into the entorhinal, lingual, isthmus cingulate, and precuneus cortices, and also covering smaller parts of the superior, inferior, and transverse temporal cortices, insula, and LOFC cortices. A small area of relations between hippocampal and cortical volume change being significantly weaker than mean cortical change was also observed around the central sulcus. As such, weaker relationships may be hard to interpret in a developmental perspective given the select age range studied (see below), our focus here is on areas of relationships stronger than mean cortical change. For the right hemisphere, weaker hippocampal–cortical change relationships were seen, partly overlapping those of the left hemisphere in the parahippocampal gyrus, but as these did not survive corrections for multiple comparisons, only the uncorrected results are shown in Supplementary Figure 2.

For the basal ganglia structures, a much more anterior pattern of relationships among cortical–subcortical volume changes was observed. As can be observed from Figure 3, caudate volume change for each hemisphere was bilaterally related to cortical volume change stronger than the mean in the ipsilateral hemisphere in all (left) or most (right) of the rostral anterior cingulate,

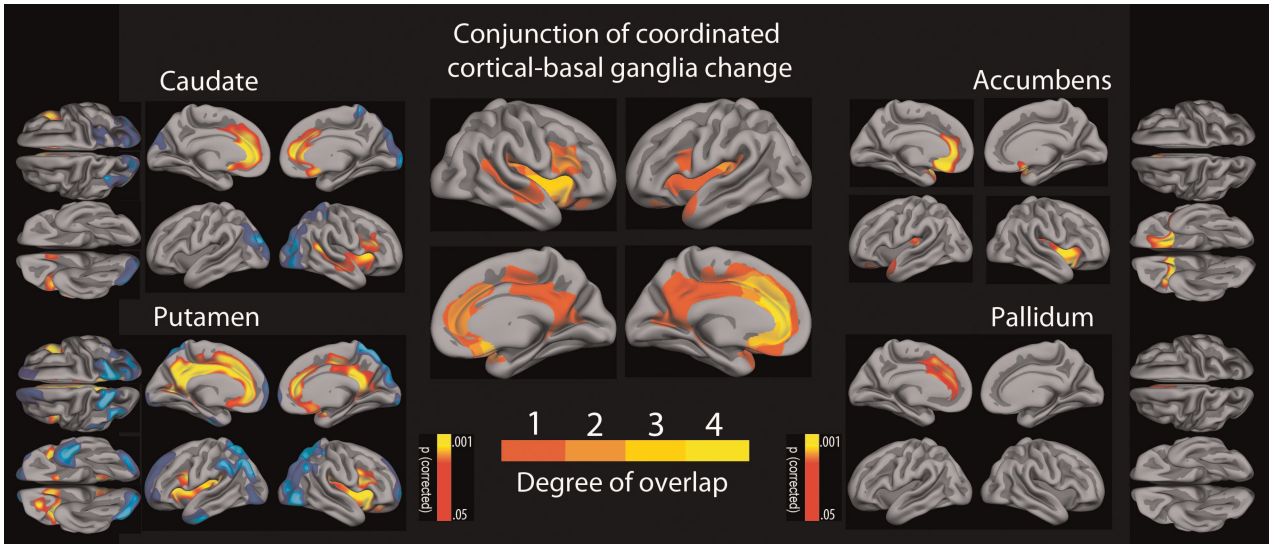

Figure 3. Coordinated basal ganglia-cortical change and conjunctions among structures. Volume change for each of the basal ganglia structures, caudate, putamen, pallidum, and accumbens area was analyzed in relation to cortical volume change across the brain surface, with sex, age, interval between baseline, and follow-up, as well as mean cortical change, as covariates. The results were corrected for multiple comparisons by Monte Carlo simulations, and only clusters with a cluster-wise $P < 0.05$ were shown. Red-yellow colors denote relationships significantly stronger than the mean ($P < 0.05$–0.001), while blue-cyan colors indicate relationships significantly weaker than the mean ($P < 0.05$ –0.001). For each vertex, the number of relationships significantly stronger than the mean across the 4 structures were counted, color-coded, and projected onto a common semi-inflated template brain.

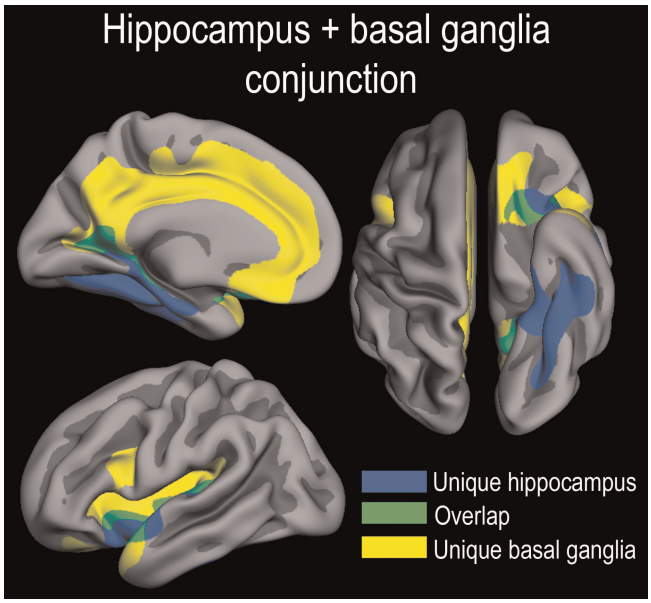

Figure 4. Conjunction of hippocampus and basal ganglia cortical relationships. Conjunction of significant relationships stronger than the mean between hippocampal and cortical change, and between basal ganglia and cortical change. As can be seen, only minute overlaps (green area) between hippocampal–cortical (blue area) and basal ganglia-cortical (yellow area) relationships are evident.

extending into the caudal anterior cingulate, medial orbitofrontal, and superior frontal cortices. Additional lateral positive relationships were observed for the right caudate and right cortical volume change in the rostral middle frontal, parstriangularis, parsopercularis, lateral orbitofrontal, insula, superior and middle temporal cortices, banks of the superior temporal sulcus, and inferior parietal cortices, bordering onto the supramarginal cortices. For the putamen, largely overlapping, but more extended relationships were seen. Medially, relationships between putamen and cortical change were covering virtually all parts of the cingulate, and part of the superior frontal and lateral orbitofrontal cortices for both the left and right hemisphere. Volume changes in larger parts of the precuneus as well as paracentral and pericalcarine cortices, and part of the cuneus were also related to putamen volume change in both hemispheres, in addition to part of the lingual cortex in left hemisphere. Laterally, extended relationships were seen for both hemispheres in the insula, lateral orbitofrontal, parstriangularis, and parsopercularis cortices, extending into the caudal middle frontal, pre- and postcentral, as well as supramarginal cortices. Pallidal volume change was significantly related to rostral and caudal anterior cingulate, as well as superior frontal cortical volume change in the left hemisphere only. Volume change of the accumbens area showed left hemisphere relationships with rostral and caudal anterior cingulate, medial orbitofrontal, and superior frontal cortical volume change. In the right hemisphere, relationships for accumbens were observed in the medial orbitofrontal cortex and the insula cortices. Some areas of negative relationships between cortical and basal ganglia structures volume changes were also observed. With the exception of the putamen for which relationships weaker than the mean were also observed in the prefrontal cortices, these were all centered on posterior cortices, especially in the occipital lobe.

As can be seen from Figure 3, overlap among positive relationships between cortical and subcortical volume change was observed among all basal ganglia structures in the left hemisphere in the rostral and caudal anterior cingulate and superior frontal cortices medially. As relationships for the pallidum did not survive corrections in the right hemisphere, no other overlapping patterns for all basal ganglia structures were observed. Overlap patterns among caudate, putamen, and accumbens were seen in parts of the anterior cingulate, medial orbitofrontal, and superior frontal cortices bilaterally and in the right hemisphere insula.

Finally, as can be seen from Figure 4, there was almost no overlap between hippocampus and basal ganglia structures in patterns of cortical–subcortical change stronger than mean cortical change.

Discussion

The present results show that patterns of cortical–subcortical development as assessed by morphometric MRI in part map on to segregated neural circuits, but also point to overlap in maturational cortical–subcortical patterns. The findings of nonoverlap imply that, to some extent, structural convergence and integration occurs within each of the identified segregated circuits (Alexander et al. 1990) also at the macrostructural level, to be discussed further below. We hypothesized that the strongest relationships of hippocampal and basal ganglia change would outline major established circuits for episodic memory and executive function (Alexander et al. 1990; Shah et al. 2012), respectively. Analyses controlling for mean cortical change indicated unique relationships between hippocampal volume change and cortical volume change in the entorhinal, parahippocampal, fusiform, lingual, isthmus cingulate, inferior parietal, and pericalcarine cortices in the left hemisphere. These relationships did not at all overlap with those of caudate and cortical volume change in development, which were restricted to anterior areas of the cingulate and frontal cortices medially, and involved lateral areas only for the right hemisphere. Neither did they overlap with cortical areas with relationships to pallidal change. Overall, overlap among hippocampus and basal ganglia cortical volume change relationships was limited, and restricted to an area of relationship in a small part of the parahippocampal, isthmus cingulate, and precuneus cortices medially, as well as small sections of the insula, transversetemporal/superior temporal, and orbitofrontal cortices in the left hemisphere. This pattern of segregated cortico-subcortical volume change relationships in part corresponds to segregation of circuits identified in previous research (Alexander et al. 1990; Shah et al. 2012).

However, overlap among patterns of change across basal ganglia structures was more widespread, with caudate, putamen, pallidum, and accumbens volume change all significantly related to more anterior cortical volume change, especially in the anterior cingulate, where patterns converged across all basal ganglia structures in the left hemisphere. Caudate volume change was confirmed to relate to prefrontal cortical volume changes, including the anterior cingulate and DLPFC. However, caudate relationships specific to medial parietal structures, for example, precuneus did not appear, but relationships with volume change in right inferior parietal and temporal cortices were observed.

According to the "segregated circuits" hypothesis, structural convergence and functional integration occur primarily "within" segregated circuits, not "between" them (Alexander et al. 1990).

Based on this, one would expect maturation of the brain to proceed along structural circuits in childhood and adolescence, with different parts of the same circuit changing in concert. Thus, one would expect change within a circuit to be more highly correlated than change across circuits. However, direct testing of this hypothesis has hardly been done. Recent exceptions are studies demonstrating coordinated anatomical change within the cortex in development (Raznahan, Lerch, et al. 2011; Alexander-Bloch et al. 2013). Maturational couplings in cortico-subcortical circuits are largely unstudied, the one exception known to us being identification of association between amygdalar volume and cerebral cortical thickness in several prefrontal areas as well as the precuneus (Albaugh et al. 2013). In that study, including healthy youths, the correlations were inverse, in line with their finding that amygdalar volume was positively related to age. As the subcortical structures studied here showed negative associations with age, as did regional cortical volume, it is not surprising that currently observed cortico-subcortical relationships were positive. Areas where relationships among cortical-subcortical changes were significantly lower than mean cortical change were also observed, primarily in the posterior cortices, centered in occipital areas. Given the age range of the present sample starting at 8 years, we find it likely that this is in part due to much maturation of these areas going on at an age prior to that of the current study (Gogtay et al. 2004), while other areas of the cortex and subcortical volumes show prolonged maturation (Østby et al. 2009; Tamnes et al. 2013). The areas where relationships among putamen and prefrontal cortical changes were weaker than the mean cortical change may in part relate to a somewhat different rate of change in the putamen with age compared with the other basal ganglia structures (Tamnes et al. 2013). However, these weaker than mean relationships may be complex, and we believe their correct interpretation would require a wider age range than that in the present study.

The present results indicate that maturational changes across subcortical and cortical regions in part follow specific macrostructural circuits as exemplified by the observed relationships between hippocampal change and the posterior cortical sections of the Papez circuit, and the correlations between basal ganglia and prefrontal cortical change. However, there was also some overlap between maturational couplings across these circuits and, to some extent, areas previously identified to correlate with amygdalar volume (Albaugh et al. 2013). Some of this may be attributable to partly common cortical couplings, as the general, almost global development of the cerebral cortex in this age range (Tamnes et al. 2010) was controlled for.

Cortical thickness is known to show an overall decrease with age in school years and beyond in MRI studies, likely related to positive processes such as pruning and/or intracortical myelination (Tamnes et al. 2010, 2013). For cortical volume, regional variability is seen with a mix of increases and decreases early on, but in the second decade of life, the picture is dominated by decreases also for cortical volume (Brown et al. 2012). Likewise, monotonous developmental decrease has been observed for basal ganglia volumes (Østby et al. 2009). A more complex age relationship has been observed for the hippocampus (Østby et al. 2009; Uematsu et al. 2012), including a somewhat more protracted growth when controlling for total brain volume, but the mean cross-sectionally estimated change also here is in terms of volume reduction in adolescence (Østby et al. 2009), with monotonous decrease within the present age range (Tamnes et al. 2013). The fact that these macrostructural developmental changes occur in concert in partly segregated subcortical–cortical circuits, may speak of coordinated pruning and myelination within these circuits. Importantly, regional specificity of spinogenesis, synaptogenesis, and pruning among cortical areas has been shown (Huttenlocher 1990; Huttenlocher and Dabholkar 1997; Elston et al. 2009). There is at present limited knowledge about the exact relationship between cellular and molecular changes and MRI measures, but the present findings underscore that regionally and functionally specific changes in part can be identified also at a macrostructural neuroanatomical level.

Why would hippocampal and pallidal change and cortical change be less related in the right hemisphere? We can think of no reason to expect hemispheric differences in coordination of hippocampal and pallidal and cortical change specifically. Rather, the reason for the weak relationship may be seen in terms of relatively little change in the hippocampus and pallidum, as evident from Table 1. Hippocampal change appears, if anything, to be even less in the right hemisphere, and so the possibility of detecting relationships is limited here. In line with previous literature, both subcortical and cortical maturation on average take the form of volume reductions in this age range and in this sample, which was confined to participants in late childhood, adolescence, and young adulthood (Tamnes et al. 2013).

Limitations, Further Research, and Conclusions

The present study is not sufficiently powered to adequately address the issue of possible sex and age group-specific differences in subcortical–cortical patterns of change. In addition, change was measured across only 2 time-points, which may yield less accurate change measures than mapping change over multiple time-points. Further research should also aim to map the maturation of these circuits onto the cognitive behavioral development of the functions they control, that is, episodic memory and executive function. The present findings show that morphometric MRI analyses can yield a window into the ongoing coordinated maturation of select neural circuits.

Supplementary Material

Supplementary can be found at: http://www.cercor.oxfordjournals.org/.

Funding

This work was supported by grants from the Norwegian Research Council (to K.B.W.), the University of Oslo (to KBW and AMF), the Department of Psychology,University of Oslo, and the US–Norway Fulbright Foundation (to CKT).

Notes

We thank all participants and their families. *Conflict of Interest:* A.M.D. is a founder and holds equity in CorTechs Labs, Inc., and also serves on the Scientific Advisory Board. The terms of this arrangement have been reviewed and approved by the University of California San Diego, in accordance with its conflict of interest policies.

References

Albaugh MD, Ducharme S, Collins DL, Botteron KN, Althoff RR, Evans AC, Karama S, Hudziak JJ, Brain Development Cooperative Group. 2013. Evidence for a cerebral cortical thickness network

anti-correlated with amygdalar volume in healthy youths: implications for the neural substrates of emotion regulation. Neuroimage. 71:42–49.
Alexander GE, Crutcher MD, DeLong MR. 1990. Basal ganglia-thalamocortical circuits: parallel substrates for motor, oculomotor, "prefrontal" and "limbic" functions. Prog Brain Res. 85:119–146.
Alexander GE, DeLong MR, Strick PL. 1986. Parallel organization of functionally segregated circuits linking basal ganglia and cortex. Annu Rev Neurosci. 9:357–381.
Alexander-Bloch A, Raznahan A, Bullmore E, Giedd J. 2013. The convergence of maturational change and structural covariance in human cortical networks. J Neurosci. 33:2889–2899.
Brain Development Cooperative Group. 2012. Total and regional brain volumes in a population-based normative sample from 4 to 18 years: the NIH MRI Study of Normal Brain Development. Cereb Cortex. 22:1–12.
Brown TT, Kuperman JM, Chung Y, Erhart M, McCabe C, Hagler DJ Jr, Venkatraman VK, Akshoomoff N, Amaral DG, Bloss CS et al. 2012. Neuroanatomical assessment of biological maturity. Curr Biol. 22:1693–1698.
Desikan RS, Segonne F, Fischl B, Quinn BT, Dickerson BC, Blacker D, Buckner RL, Dale AM, Maguire RP, Hyman BT et al. 2006. An automated labeling system for subdividing the human cerebral cortex on MRI scans into gyral based regions of interest. Neuroimage. 31:968–980.
Disbrow EA, Sigvardt KA, Franz EA, Turner RS, Russo KA, Hinkley LB, Herron TJ, Ventura MI, Zhang L, Malhado-Chang N. 2013. Movement activation and inhibition in Parkinson's disease: a functional imaging study. J Parkinson Dis. 3:181–192.
Elston GN, Oga T, Fujita I. 2009. Spinogenesis and pruning scales across functional hierarchies. J Neurosci. 29:3271–3275.
Evans AC. 2013. Networks of anatomical covariance. Neuroimage. 80:489–504.
Fischl B, Dale AM. 2000. Measuring the thickness of the human cerebral cortex from magnetic resonance images. Proc Natl Acad Sci USA. 97:11050–11055.
Fischl B, Salat DH, Busa E, Albert M, Dieterich M, Haselgrove C, van der Kouwe A, Killiany R, Kennedy D, Klaveness S et al. 2002. Whole brain segmentation: automated labeling of neuroanatomical structures in the human brain. Neuron. 33:341–355.
Fischl B, Sereno MI, Dale AM. 1999. Cortical surface-based analysis. II: inflation, flattening, and a surface-based coordinate system. Neuroimage. 9:195–207.
Fischl B, Sereno MI, Tootell RB, Dale AM. 1999. High-resolution intersubject averaging and a coordinate system for the cortical surface. Hum Brain Mapp. 8:272–284.
Fischl B, van der Kouwe A, Destrieux C, Halgren E, Segonne F, Salat DH, Busa E, Seidman LJ, Goldstein J, Kennedy D et al. 2004. Automatically parcellating the human cerebral cortex. Cereb Cortex. 14:11–22.
Fjell AM, Walhovd KB, Fennema-Notestine C, McEvoy LK, Hagler DJ, Holland D, Brewer JB, Dale AM. 2009. One-year brain atrophy evident in healthy aging. J Neurosci. 29:15223–15231.
Ghetti S, Bunge SA. 2012. Neural changes underlying the development of episodic memory during middle childhood. Dev Cogn Neurosci. 2:381–395.
Gogtay N, Giedd JN, Lusk L, Hayashi KM, Greenstein D, Vaituzis AC, Nugent TF 3rd, Herman DH, Clasen LS, Toga AW et al. 2004. Dynamic mapping of human cortical development during childhood through early adulthood. Proc Natl Acad Sci USA. 101:8174–8179.
Haber SN, Knutson B. 2010. The reward circuit: linking primate anatomy and human imaging. Neuropsychopharmacology. 35:4–26.
Hagler DJ Jr, Saygin AP, Sereno MI. 2006. Smoothing and cluster thresholding for cortical surface-based group analysis of fMRI data. Neuroimage. 33:1093–1103.
Hayasaka S, Nichols TE. 2003. Validating cluster size inference: random field and permutation methods. Neuroimage. 20:2343–2356.
Holland D, Dale AM. 2011. Nonlinear registration of longitudinal images and measurement of change in regions of interest. Med Image Anal. 15:489–497.
Holland D, McEvoy LK, Dale AM. 2012. Unbiased comparison of sample size estimates from longitudinal structural measures in ADNI. Hum Brain Mapp. 33:2586–2602.
Huttenlocher PR. 1990. Morphometric study of human cerebral cortex development. Neuropsychologia. 28:517–527.
Huttenlocher PR, Dabholkar AS. 1997. Regional differences in synaptogenesis in human cerebral cortex. J Comp Neurol. 387:167–178.
Jovicich J, Czanner S, Greve D, Haley E, van der Kouwe A, Gollub R, Kennedy D, Schmitt F, Brown G, Macfall J et al. 2006. Reliability in multi-site structural MRI studies: effects of gradient non-linearity correction on phantom and human data. NeuroImage. 30:436–443.
Lenroot RK, Giedd JN. 2006. Brain development in children and adolescents: insights from anatomical magnetic resonance imaging. Neurosci Biobehav Rev. 30:718–729.
Lerch JP, Worsley K, Shaw WP, Greenstein DK, Lenroot RK, Giedd J, Evans AC. 2006. Mapping anatomical correlations across cerebral cortex (MACACC) using cortical thickness from MRI. Neuroimage. 31:993–1003.
Lovstad M, Funderud I, Endestad T, Due-Tonnessen P, Meling TR, Lindgren M, Knight RT, Solbakk AK. 2012. Executive functions after orbital or lateral prefrontal lesions: neuropsychological profiles and self-reported executive functions in everyday living. Brain Inj. 26:1586–1598.
Milad MR, Rauch SL. 2012. Obsessive-compulsive disorder: beyond segregated cortico-striatal pathways. Trends Cogn Sci. 16:43–51.
Murphy EA, Holland D, Donohue M, McEvoy LK, Hagler DJ Jr, Dale AM, Brewer JB. 2010. Six-month atrophy in MTL structures is associated with subsequent memory decline in elderly controls. NeuroImage. 53:1310–1317.
Østby Y, Tamnes CK, Fjell AM, Westlye LT, Due-Tønnessen P, Walhovd KB. 2009. Heterogeneity in subcortical brain development: a structural magnetic resonance imaging study of brain maturation from 8 to 30 years. J Neurosci. 29:11772–11782.
Park HJ, Friston K. 2013. Structural and functional brain networks: from connections to cognition. Science. 342:1238411.
Raznahan A, Lerch JP, Lee N, Greenstein D, Wallace GL, Stockman M, Clasen L, Shaw PW, Giedd JN. 2011. Patterns of coordinated anatomical change in human cortical development: a longitudinal neuroimaging study of maturational coupling. Neuron. 72:873–884.
Raznahan A, Shaw P, Lalonde F, Stockman M, Wallace GL, Greenstein D, Clasen L, Gogtay N, Giedd JN. 2011. How does your cortex grow? J Neurosci. 31:7174–7177.
Robbins TW. 2007. Shifting and stopping: fronto-striatal substrates, neurochemical modulation and clinical implications. Philos Trans R Soc Lond B Biol Sci. 362:917–932.
Shah A, Jhawar SS, Goel A. 2012. Analysis of the anatomy of the Papez circuit and adjoining limbic system by fiber dissection techniques. J Clin Neurosci. 19:289–298.
Shepherd GM. 2013. Corticostriatal connectivity and its role in disease. Nat Rev Neurosci. 14:278–291.
Sled JG, Zijdenbos AP, Evans AC. 1998. A nonparametric method for automatic correction of intensity nonuniformity in MRI data. IEEE Trans Med Imaging. 17:87–97.
Sowell ER, Trauner DA, Gamst A, Jernigan TL. 2002. Development of cortical and subcortical brain structures in childhood and adolescence: a structural MRI study. Dev Med Child Neurol. 44:4–16.
Tamnes CK, Østby Y, Fjell AM, Westlye LT, Due-Tønnessen P, Walhovd KB. 2010. Brain maturation in adolescence and young adulthood: regional age-related changes in cortical thickness and white matter volume and microstructure. Cereb Cortex. 20:534–548.
Tamnes CK, Walhovd KB, Dale AM, Ostby Y, Grydeland H, Richardson G, Westlye LT, Roddey JC, Hagler DJ Jr, Due-Tonnessen P et al. 2013. Brain development and aging: overlapping and unique patterns of change. Neuroimage. 68:63–74.
Uematsu A, Matsui M, Tanaka C, Takahashi T, Noguchi K, Suzuki M, Nishijo H. 2012. Developmental trajectories of amygdala and hippocampus from infancy to early adulthood in healthy individuals. PLoS One. 7:e46970.
Wechsler D. 1999. Wechsler Abbreviated Scale of Intelligence (WASI). San Antonio (TX): The Psychological Corporation.